Clim Dyn (2006) 27:831–849
DOI 10.1007/s00382-006-0166-0

Evaluation of different freshwater forcing scenarios for the 8.2 ka BP event in a coupled climate model

A. P. Wiersma · H. Renssen · H. Goosse · T. Fichefet

Received: 19 January 2006 / Accepted: 2 June 2006 / Published online: 22 July 2006

Abstract To improve our understanding of the mechanism causing the 8.2 ka BP event, we investigated the response of ocean circulation in the ECBilt-CLIO-VECODE (Version 3) model to various freshwater fluxes into the Labrador Sea. Starting from an early Holocene climate state we released freshwater pulses varying in volume and duration based on published estimates. In addition we tested the effect of a baseline flow (0.172 Sv) in the Labrador Sea to account for the background-melting of the Laurentide ice-sheet on the early Holocene climate and on the response of the overturning circulation. Our results imply that the amount of freshwater released is the decisive factor in the response of the ocean, while the release duration only plays a minor role, at least when considering the short release durations (1, 2 and 5 years) of the applied freshwater pulses. Furthermore, the experiments with a baseline flow produce a more realistic early Holocene climate state without Labrador Sea Water formation. Meltwater pulses introduced into this climate state produce a prolonged weakening of the overturning circulation compared to an early Holocene climate without baseline flow, and therefore less freshwater is needed to produce an event of similar duration.

A. P. Wiersma (✉) · H. Renssen
Faculty of Earth and Life Sciences, Vrije Universiteit Amsterdam, De Boelelaan 1085, 1081 HV Amsterdam, The Netherlands
e-mail: ane.wiersma@falw.vu.nl

H. Goosse · T. Fichefet
Institut d'Astronomie et de Géophysique George Lemaître, Université Catholique de Louvain, Chemin du Cyclotron 2, 1348 Louvain-la-Neuve, Belgium

1 Introduction

During the early Holocene from 11.5 to 7 cal ka BP (hereafter ka BP), the remaining glacial ice-sheets melted under the warm climate conditions. Due to regional geography in North America, part of the meltwater collected in huge proglacial lakes south of the retreating Laurentide Ice-Sheet (LIS), the so-called Laurentide lakes. The remnant LIS formed a massive ice-dam, which prevented the lakes from draining into the North Atlantic Ocean (e.g. Upham 1896; Veillette 1994; Clarke et al. 2004). Between 9 and 8 ka BP, collapse of the ice-dam became unavoidable, thereby releasing a huge amount of meltwater into the Hudson Bay.

The timing of the collapse of the ice-dam and the subsequent draining of the Laurentide lakes is estimated at ~8.47 ka BP (Barber et al. 1999), and considering dating uncertainties, this coincides with the start of the most pronounced cold period recorded in the North Atlantic area, the so called 8.2 ka BP event (e.g. Alley et al. 1997; Barber et al. 1999). Several investigators linked the two events, suggesting that the drainage of the Laurentide lakes caused the 8.2 ka BP event (e.g. von Grafenstein et al. 1998; Klitgaard-Kristensen et al. 1998; Barber et al. 1999). The proposed mechanism is that the freshwater slowed down the Meridional Overturning Circulation (MOC) by preventing dense water to sink in the North Atlantic Ocean and thereby reducing the northward heat transport to the North Atlantic region. Such a collapse of the MOC is also observed during Heinrich events (Keigwin and Lehman 1994; Elliot et al. 2002), and in modelling studies in which the modern North Atlantic is perturbed with freshwater (e.g. Stocker and Wright 1991; Manabe and Stouffer 1995, 1997; Vellinga and Wood 2002).

In recent years, widely varying estimates of the involved freshwater pulse have been published (Table 1), ranging from 0.3 to 5.0×10^{14} m^3. A comprehensive study by Leverington et al. (2002) produced an estimate of 1.63×10^{14} m^3 based on bathymetric models. To constrain the magnitude and duration of the flood, Clarke et al. (2004) simulated flood hydrographs for lake discharge for different drainage routes and from different filling levels, and found that the draining of the Laurentide lakes had a typical duration of less than a year with peak discharge rates up to 9 Sv (1 Sv = 10^6 m^3/s). The total water volume available for drainage for the different drainage routes ranged from 0.40×10^{14} to 1.51×10^{14} m^3. Surprisingly, several hydrographs revealed a multi-pulse structure and in none of the experiments the lakes drained completely. Even in the scenario with the largest drained volume, less than half of the total available volume of the lake drained. However, Clarke et al. (2004) only accounted for subglacial outburst flooding. They could not rule out physical failure of the LIS, collapse of the ice roof of subglacial channels and a supraglacial flood mechanism as additional freshwater sources (Clarke et al. 2005; Sharpe 2005). Consequently, the released volume and drainage duration may have been larger than suggested by Clarke et al. (2004).

Complete or partial physical failure of the LIS would have led to the release of an additional volume of ice, in addition to the lake water. Based on maps of Dyke and Prest (1989) and von Grafenstein et al. (1998) even suggested that one third of the LIS may have been released into the Labrador Sea as floating ice and roughly estimates that 5×10^{14} m^3 of meltwater from the lakes and the ice-sheet was released. However, Törnqvist et al. (2004) showed recently that the maximum sea-level rise following the lake drainage is 1.19 m, implying that the total volume of meltwater and ice cannot have exceeded 4.3×10^{14} m^3. Still, despite this maximum constrain, the actual volume of meltwater that was released remains highly uncertain (Table 1), especially since the contribution of the LIS, from which a substantial part disappeared between 7.8 and 7.2 ^{14}C ka BP (~8.6–8.0 ka BP, Dyke 2003), is still unclear. On the floor of the Hudson Bay, however, there is evidence for drifting icebergs during the discharge: a large area with iceberg scours is present, probably originating from grounded icebergs that were mobilized by fast-flowing water (Josenhans and Zevenhuizen 1990; Dyke 2003). In addition, peaks in ice-rafted detritus (IRD) in several marine cores in the Atlantic Ocean around 8.2 ka BP (e.g. Bond et al. 2001; Moros et al. 2004) suggest the drifting of icebergs, but on the other hand these IRD peaks may also reflect the 8.2 ka BP cooling.

Table 1 Estimates of the volume of freshwater that was released during the collapse of the remnant Laurentide ice-sheet previous to 8.2 ka BP

Authors	Freshwater volume (10^{14} m^3)
von Grafenstein et al. (1998)	5
de Vernal (1997)	1.2
Leverington et al. (2002)	1.63
Barber et al. (1999)	~2
Törnqvist et al. (2004)	< 4.3
Veillette (1994)	~2.28
Clarke et al. (2004)	0.279–0.708
Modelling papers	
Bauer et al. (2004)	1.6
Renssen et al. (2001)	4.67
This paper	1.63
	3.26
	4.89

When the Laurentide lakes drained in the early Holocene, the Atlantic Ocean circulation was different from the present. From micropaleontological data and stable isotopes on both planktonic and benthic foraminifera, Hillaire-Marcel et al. (2001) concluded that deep-water formation in the Labrador Sea was absent during the last glacial cycle and only started at 7 ka BP. This means that Labrador Sea Water (LSW) formation was probably absent at the time of the lake discharge around 8.47 ka BP. In a modelling study focused on Holocene North Atlantic deep-water formation, Renssen et al. (2005a) performed an experiment forced only by changes in orbital forcing and atmospheric trace gas concentrations for the last 9,000 years. They found that the LSW formation was weaker in the early Holocene than at present. However, in this study, a complete shutdown of LSW formation in the early Holocene was not simulated under the imposed forcings. This was probably related to a relatively high surface salinity in the Labrador Sea in the early Holocene, since the effect of the melting LIS (i.e. the associated freshwater flux) was not included in the experiments (Renssen et al. 2005a). The latter conclusion is consistent with Cottet-Puinel et al. (2004), who simulated an early Holocene shutdown of

LSW formation in a transient model run including the freshwater runoff of the LIS.

Recently, several attempts have been made to simulate the 8.2 ka BP event. Renssen et al. (2001, 2002) introduced pulses of freshwater into the Labrador Sea under early Holocene boundary conditions, using Version 2 of the ECBilt-CLIO climate model. A scenario with a fresh water pulse of 4.67×10^{14} m^3 during 20 years resulted in a cold period comparable to the 8.2 ka BP event as reconstructed from proxy-evidence (Wiersma and Renssen 2006). Later, Bauer et al. (2004) simulated the event with the CLIMBER-2 model, by introducing a 2-year pulse of 1.6×10^{14} m^3 fresh-water into the North Atlantic Ocean between 50 and 70°N, also in an early Holocene climate. The experiment produced a short-term cooling of 20-year duration. Additionally, Bauer et al. (2004) experimented with a freshwater flux representing the background melting LIS (the so-called baseline flow). This baseline flow weakened the MOC, which promoted collapse of the NADW formation after introducing the same freshwater pulse of 1.6×10^{14} m^3, in some scenarios resulting in a cooling lasting two centuries.

Altogether, the specific conditions that probably led to the 8.2 ka BP event remain uncertain. The latest estimates suggest that the released meltwater volume during the collapse of the LIS was between 0.279×10^{14} (Clarke et al. 2004) and 4.3×10^{14} m^3 (Törnqvist et al. 2004) and that the release duration was short, and estimates range from between 1 and 10 years (Licciardi et al. 1999) to even less than a year (Barber et al. 1999; Clarke et al. 2004).

Knowing these specific conditions for the 8.2 ka BP event provides crucial information on the sensitivity of the MOC to perturbations (e.g. Schlessinger 2005). In this study, we investigate the influence of varying magnitude and duration of the freshwater pulse on the response of the MOC in Version 3 of the ECBilt-CLIO-VECODE model while previous modelling studies experimented with a constant volume (Bauer et al. 2004), and unrealistic release durations (i.e. 10 years or more, Renssen et al. 2001, 2002). In contrast to the previous study of Bauer et al. (2004), our model allows us to investigate the spatial response of the ocean to this forcing. Furthermore, we investigate the influence of a baseline flow due to the LIS melting on the early Holocene climate as in Bauer et al. (2004), and its influence on the MOC's response to the varying freshwater perturbations. This provides information on the sensitivity of the MOC to these factors (i.e. freshwater volume, discharge rate, baseline flow or initial conditions) as well as their share in the evolution of the 8.2 ka BP event.

2 The ECBilt-CLIO-VECODE model

We have performed our experiment with Version 3 of the ECBilt-CLIO-VECODE model, a global, three-dimensional climate model of intermediate complexity. The model consists of an oceanic, sea-ice, atmospheric and vegetation component. The atmospheric component is Version 2 of ECBilt, a spectral quasi-geostrophic model with three levels and T21-resolution developed at the Koninklijk Nederlands Meteorologisch Instituut (KNMI) (Opsteegh et al. 1998). ECBilt includes a representation of the hydrological cycle and simple parameterizations of the diabatic heating processes. Cloudiness is prescribed according to present-day climatology (Rossow et al. 1996) and a dynamically passive stratospheric layer is included. As an extension to the quasi-geostrophic equations, an estimate of the neglected terms in the vorticity and thermodynamic equations is incorporated as a temporally and spatially varying forcing (Opsteegh et al. 1998). This forcing is computed from the diagnostically derived vertical motion field, leading to a considerable improvement of the simulation of the Hadley circulation and resulting in a drastic improvement of the strength and position of the jet stream and transient eddy activity. The hydrological cycle is closed over land by using a bucket for soil moisture. Each bucket is connected to a nearby oceanic gridcell to define river runoff. Accumulation of snow occurs in case of precipitation in areas with below 0°C surface temperature. Greenhouse gases are incorporated directly into the model, and not as equivalent CO_2.

The sea-ice—ocean component is CLIO (Goosse and Fichefet 1999), a primitive-equation free-surface ocean general circulation model (OGCM) (Deleersnijder and Campin 1995; Campin and Goosse 1999) coupled to a comprehensive sea-ice model with a representation of both thermodynamic and dynamic processes (Fichefet and Morales Maqueda 1997) that was developed at Université Catholique de Louvain (Goosse and Fichefet 1999). The ocean model includes a detailed formulation of boundary layer mixing based on Mellor and Yamada's (1982) level-2.5 turbulence closure scheme (Goosse et al. 1999) and a parameterization of density-driven down-slope flows (Campin and Goosse 1999). The sea-ice model takes into account the heat capacity of the snow—ice system, the storage of latent heat in brine pockets trapped inside the ice, the effect of the sub-grid scale snow and ice thickness distributions on sea-ice thermodynamics, the formation of snow ice under excessive snow loading and the existence of leads within the ice cover. Ice dynamics are calculated by assuming that sea ice behaves as a two-dimensional viscous-plastic continuum. The horizontal resolution of CLIO is 3° latitude by 3° longitude, and there are 20 unequally spaced vertical levels in the ocean.

The vegetation module VECODE, a dynamic global vegetation model developed at the Potsdam Institut für Klimafolgenforschung (PIK) (Brovkin et al. 2002), was recently coupled to ECBilt-CLIO. VECODE simulates dynamics of two main terrestrial plant functional types, trees and grasses, as well as desert (bare soil), in response to climate change. Within ECBilt-CLIO-VECODE, simulated vegetation changes affect only the land-surface albedo, and have no influence on other processes, e.g. evapotranspiration or roughness length.

Compared to earlier versions, the present model simulates a climate, i.e. closer to modern observations. The most important improvements in the new version are a new land surface scheme that takes into account the heat capacity of the soil, and the use of isopycnal diffusion as well as the Gent and McWilliams parameterization to represent the effect of meso-scale eddies in the ocean (Gent and McWilliams 1990). The climate sensitivity of ECBilt-CLIO is about 0.5°C/(W/m^2), which is at the lower end of the range [typically 0.5–1°/(W/m^2)] found in most coupled climate models (Cubasch et al. 2001). The only flux correction required in ECBilt-CLIO is an artificial reduction of precipitation over the Atlantic and Arctic Oceans, and a homogeneous distribution of the removed amount of freshwater over the Pacific Ocean (Goosse et al. 2001).

Version 3 of the ECBilt-CLIO model was recently applied by Knutti et al. (2004) to study the impact of freshwater discharges on the climate during the last glacial stage, but also in experiments investigating Holocene climate evolution (e.g. Renssen et al. 2005a, b) and in studies covering the last millennium (e.g. Goosse et al. 2005). Version 2 of the model was used earlier for the simulation of the 8.2 ka BP event (Renssen et al. 2001, 2002) and a variety of other applications, i.e. to simulate aspects of the present-day climate (Goosse et al. 2001, 2003), natural variability of the modern climate (Goosse et al. 2002) and future climate evolution (Goosse and Renssen 2001; Schaeffer et al. 2002). The improvements and updates in model Version 3 lead to important differences with model Version 2 that was used by Renssen et al. (2001, 2002) to study the 8.2 ka BP event. In contrast to Version 2, when run with modern forcings, the new version simulates deep convection in the Labrador Sea in agreement with observational estimates, and also the strength of overturning in the Greenland–Iceland–Norwegian (GIN) seas is greatly reduced to more realistic values of <4 Sv (compared to ~17 Sv in Version 2). Under pre-industrial climate conditions, the maximum of the North Atlantic overturning circulation is in present model version ~27 and ~13 Sv of NADW is exported southward at 20°S and the meridional heat transport at 30°S is 0.33 PW.

More detailed information about ECBilt-CLIO-VECODE and its climatology can be found on the models website (http://www.knmi.nl/onderzk/CKO/ecbilt.html). In particular, a description of the differences between ECBilt-CLIO Versions 2 and 3 is also available on this website (http://www.knmi.nl/onderzkCKO/differences.html).

3 Early Holocene reference climate

3.1 Experimental setup

To simulate the early Holocene climate state, we adjusted several boundary conditions to their 8.5 ka BP values. Atmospheric greenhouse gas concentrations were adjusted to their 8.5 ka BP values inferred from ice-cores analyses by Raynaud et al. (2000) (i.e. CO_2 = 261 ppbv, CH_4 = 650 ppbv and N_2O = 270 ppbv). Orbital parameters were adjusted to represent 8.5 ka BP insolation conditions (Berger and Loutre 1991; Berger 1992), with higher insolation values in the northern hemisphere in boreal summer and lower insolation values in boreal winter compared to present-day values. We accounted for a remnant LIS by lowering surface albedo and increasing elevation of the concerned gridcells according to the Peltier (1994) reconstruction (assuming a deglaciated Hudson Bay).

The model was run for 850 years with these 8.5 ka BP boundary conditions until it reached a quasi-equilibrium in the deepest ocean layer (dT/dt < 0.0002°C/100 years). The results from the last 100 years of this experiment are used in this paper to analyse the early Holocene quasi-equilibrium climate state without baseline flow (EHequi).

In addition to this early Holocene quasi-equilibrium state, we investigated the effect of the background LIS melting by introducing a baseline flow (Bauer et al. 2004) into the Labrador Sea (ECBilt gridcell centred around 53.5°N and 50.5°W), starting from EHequi. Before the lake discharge this baseline flow is reconstructed to have amounted to 0.15 Sv, increasing to 0.172 Sv after the discharge (Licciardi et al. 1999; Teller et al. 2002). We used the latter value as the baseline flow magnitude during the course of this experiment. The model was run for 900 years in this configuration until the temperature of the deepest ocean layer was quasi-stable (dT/dt < 0.01°C/100 years). The results from the last 100 years of this experiment are used in this paper to analyse the early Holocene quasi-equilibrium climate state with a baseline flow (EHBLF). It should be noted that experiments including a baseline flow into the Labrador Sea are not considered equilibrium climate states, since we add water to the ocean, which slowly reduces salinity. However, this is analogous to the early Holocene situation of a melting remnant ice-sheet. A consequence is, that in the EHBLF experiments, the global mean ocean salinity is 0.1 psu lower than in the EHequi experiments at the end of the early Holocene equilibrium runs.

3.2 Impact of the baseline flow on the early Holocene climate

In the EHequi experiments, deep convection occurs in the Nordic Seas, the Irminger Sea and in the Labrador Sea (Fig. 1a). In this state, the maximum North Atlantic overturning is 24 Sv (Fig. 1b). This state is very close to the one simulated by the model for pre-industrial conditions, with only a weak decrease of the intensity of the MOC for the early Holocene. The introduction of the baseline flow in the early Holocene climate causes the Labrador Sea convection depth to greatly decrease by more than 500 m in February (Fig. 1c, e) and subsequently LSW formation to almost shutdown. This is consistent with proxy-data suggesting no LSW formation during the early Holocene (Hillaire-Marcel et al. 2001). The near absence of LSW formation as a result of the baseline flow causes a reduction in maximum North Atlantic overturning of more than 7 Sv and a shallower NADW cell (Fig. 1d, f). Overturning in the GIN Seas is almost unaffected by the baseline freshwater input in the Labrador Sea, and decreases from 3.3 Sv in EHequi to 3.2 Sv in EHBLF. In terms of NADW export, only 10.8 Sv crosses at 20°S in EHBLF compared to 13.8 Sv in EHequi.

The reduced overturning in the North Atlantic leads to a decrease in meridional heat transport, at 30°S a decrease of 21% from 0.33 PW in EHequi to 0.26 PW in EHBLF. Since deep convection almost ceased in the Labrador Sea, the effect of this decreased heat flux is mostly visible here, leading to ~2°C cooler conditions (Fig. 2).

4 Freshwater perturbation experiments

4.1 Experimental setup

We perturbed both early Holocene climate states (EHequi and EHBLF) by releasing freshwater pulses into the Labrador Sea (ECBilt gridcell centred around 53.5°N and 50.5°W), varying in volume and duration. It is assumed that the temperature of the discharged freshwater is identical to the sea surface temperature at the spot of discharge. Table 2 summarizes the different performed experiments schematically. The ‘‘single volume’’ of 1.63×10^{14} m^3 is based on the estimate by Leverington et al. (2002). The ‘‘double volume’’ corresponds to a total volume of 3.26×10^{14} m^3 to take into account that some ice could have been released too because of the freshwater discharge. Note that the ‘‘triple volume’’ scenario of 4.89×10^{14} m^3 is an amount that even exceeds the maximum set by Törnqvist et al. (2004) and is not realistic for an 8.2 ka BP event simulation, but it is used here to assess how close the Atlantic overturning is to a collapse or shift to an intermediate stable state. It is also near the value used by Renssen et al. (2001, 2002). Every experiment (with same volume and duration of the freshwater pulse) was performed five times (i.e. five ensemble members), each with different initial conditions, which were obtained by taking samples every 10 years from a continuation of the early Holocene experiment. The ensemble members have been labelled ‘‘a’’ to ‘‘e’’. After the freshwater perturbation, the experiments were continued in the configuration of before the pulse.

In the next paragraphs, we will first describe the results of the freshwater perturbation experiments of the EHequi climate state, then the freshwater perturbations of the EHBLF climate state and finish with a comparison between the experiments. We describe the ensemble mean of the different experiments, implying that the variability is averaged out and that the maximum magnitude of the different ensembles is mostly larger than the mentioned ensemble mean values.

4.2 MOC response to freshwater perturbations in EHequi

In all experiments, the maximum North Atlantic overturning weakens sharply after the introduction of the freshwater pulses (Fig. 3a–f). In contrast to earlier studies however (Renssen et al. 2001, 2002; Bauer et al. 2004), the different ensemble members show similar responses of the strength of the MOC, which suggests that the forcing implied by the freshwater does not push the MOC over a threshold that could cause a shift to an intermediate stable state. This results in a more predictable response of the strength of the MOC to the freshwater perturbations, compared to Renssen et al. (2001, 2002) and Bauer et al. (2004), where the timing of recovery from the intermediate stable was

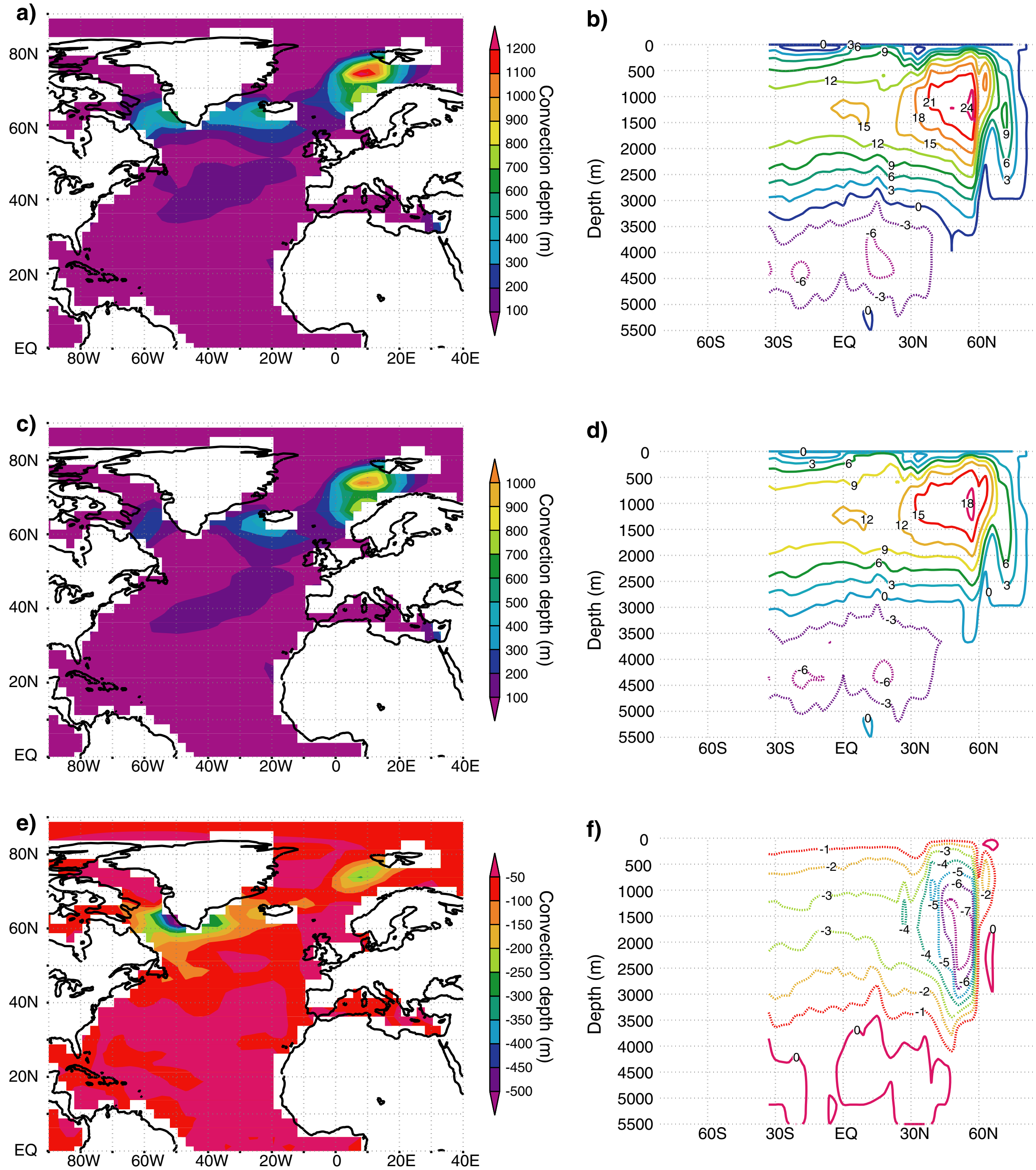

Fig. 1 Mean February convection depth (m) (*left*) and the annual mean maximum overturning streamfunction (Sv) for the initial early Holocene climate states (*right*) for **a**, **b** EHequi, **c**, **d** EHBLF and **e**, **f** the difference between the two (EHBLF minus EHequi)

unpredictable. Furthermore, the response of the strength of the MOC in experiments in which an equal volume of freshwater is released (i.e. Fig. 3a, b and d; Fig. 3c and e) is comparable, regardless of the duration of the pulse. The shape of the weakened state of the strength of the MOC in the single volume scenarios (EHequi1, EHequi2 and EHequi5) consists of an immediate sharp reduction, followed by a fast acceleration back to near-normal values around the year 125, before gradually recovering to pre-perturbed values within 100 years. This weakening leads to an average decrease in meridional heat transport at 30°S of up to 0.1 PW (30%) that gradually recovers within the same time span. In the double volume scenarios

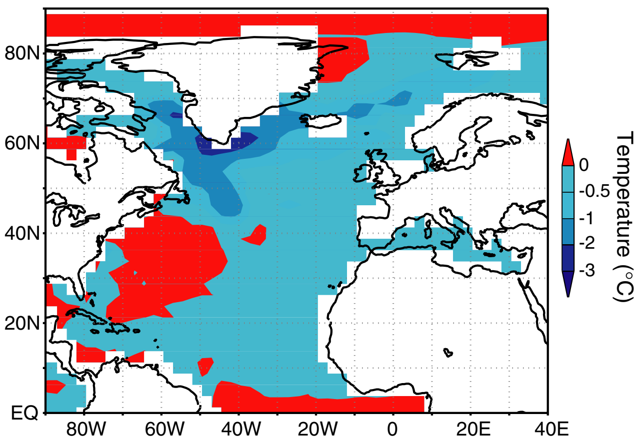

Fig. 2 Map showing the mean annual sea surface temperature anomaly (°C) of the EHBLF state compared to the EHequi state

(EHequi2d and EHequi5d), MOC strength weakens sharply again, followed by an acceleration back to values around ~23 Sv, from which the MOC strength gradually recovers back to pre-perturbed values within ~120 years after the freshwater perturbation. The meridional heat transport at 30°S is reduced by up to 0.15 PW (47%), before gradually recovering to normal values within the same time span as the strength of the MOC. In the triple volume scenario (EHequi5t), the weakening of the MOC strength behaves in a similar way as in the double volume scenarios, but lasts ~150 years and the fast acceleration stops at values of ~17 Sv before gradually recovering from this point. Meridional heat transport at 30°S is reduced by 0.18 PW (65%). In all scenarios, the reduction of the MOC strength consists of a spike that lasts around 20 years, followed by a gradual recovery of which the duration depends on the released volume and is therefore most pronounced in the double and triple scenarios. Surprisingly, the minimum value of the North Atlantic overturning strength in the different perturbation scenarios varies only moderately from ~17 Sv for the single pulse scenario to ~14 Sv for the triple pulse scenario. The probable cause for this is that in all scenarios, overturning strength decreases in the Labrador Sea and Irminger Sea during this period, and is relatively unaffected elsewhere. Therefore it appears that the different scenarios have mainly an influence on the duration of the weakening of the overturning, and less on the magnitude.

Table 2 Schematic presentation of the different freshwater perturbation experiments that were performed from the control climates of EHequi and EHBLF

Volume duration (years)	Single volume 1.63×10^{14} m^3	Double volume 3.26×10^{14} m^3	Triple volume 4.89×10^{14} m^3
1	*X*		
2	*X*	*X*	
5	*X*	*X*	*X*

All experiments consist of five ensemble members

4.3 MOC response to freshwater perturbations in EHBLF

Also in the EHBLF freshwater perturbation experiments, the maximum North Atlantic overturning strength decreases after the introduction of the freshwater pulses (Fig. 4a–f). Again, the response of the MOC is similar for the ensemble members, although in EHBLF2, EHBLF2d and EHBLF5t one ensemble member is slightly offset (Fig. 4). Main factor in the duration, magnitude and shape of the response is again freshwater volume, while the duration of the freshwater pulse is only of minor importance. In the single volume scenarios (EHBLF1, EHBLF2 and EHBLF5), MOC strength weakens sharply to values of ~15 Sv, followed by an acceleration back to values of ~18 Sv at around 25 years after the introduction of the freshwater. From this point on the MOC strength slows down again followed by a gradual recovery until ~160 years after the introduction of the freshwater pulse, after which an indistinct century-long recovery back to pre-perturbed values occurs. The average meridional heat transport in the ocean at 30°S reduces by 0.08 PW (30%) gradually recovering to normal conditions within the same time span as the MOC strength. For the double volume scenarios (EHBLF2d and EHBLF5d), the weakened MOC state lasts around 250 years coinciding with a maximum average decrease in meridional heat transport at 30°S of up to 0.13 PW (50%). The shape of the MOC strength reduction is similar to the single volume scenarios, except that the acceleration stops at values of ~16 Sv and that there is only one gradual recovery back to pre-perturbed values. The triple volume scenario (EHBLF5t) produces a weakened North Atlantic overturning state during ~330 years, coinciding with a reduced meridional heat transport at 30°S of up to 0.17 PW (65%) that gradually recovers back to normal values within the same time span. The shape of the response of the MOC consists of a spike that lasts around 25 years as in some of the experiments by Bauer et al. (2004), but in our experiments followed by a gradual recovery in all scenarios. The lowest rate of maximum overturning only varies from ~15 Sv for the single pulse scenario to ~12 Sv for the triple pulse scenario.

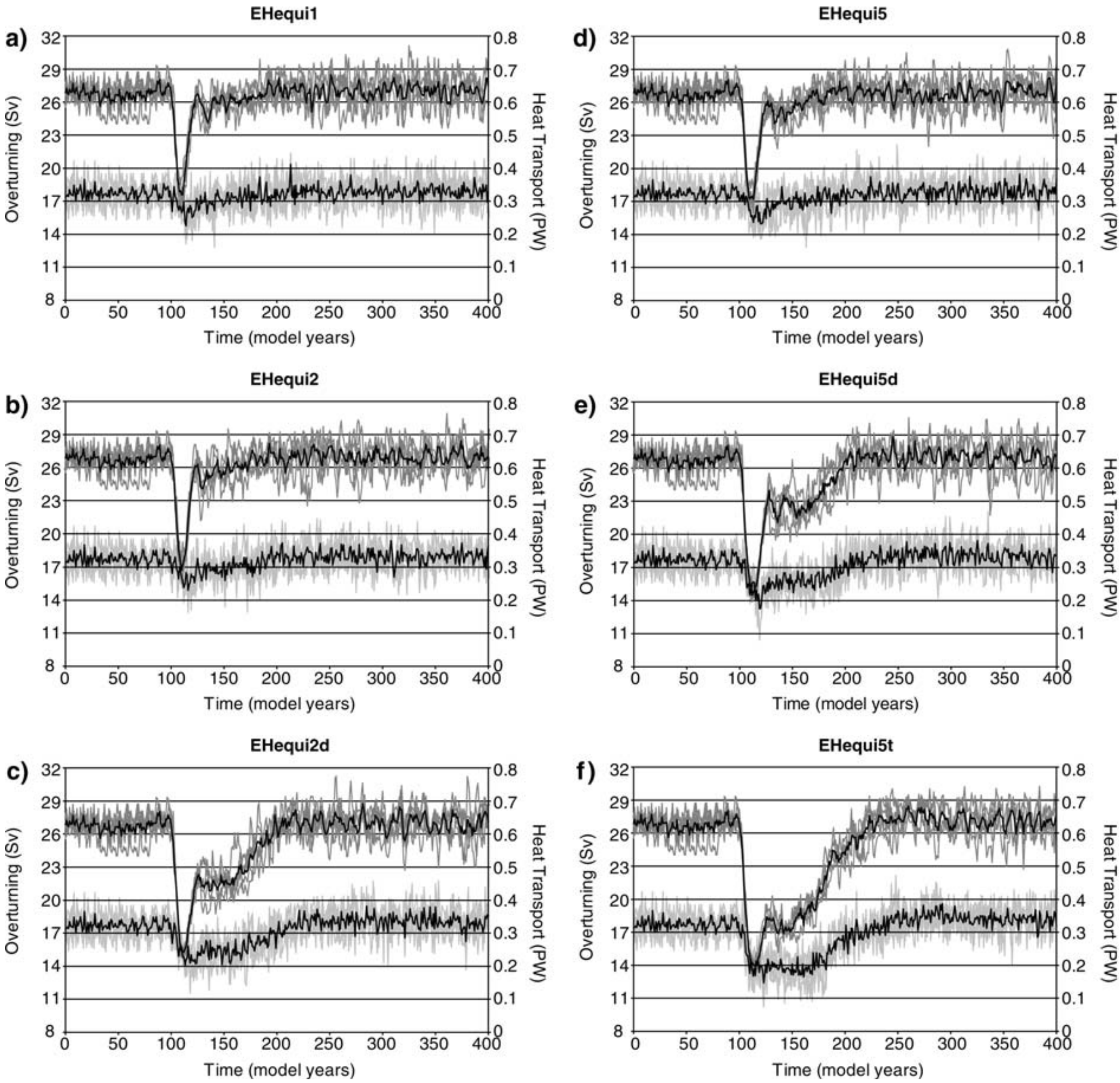

Fig. 3 Maximum North Atlantic overturning (Sv) (*upper line, dark shading, left axis*) and meridional heat transport (PW) in the oceans at 30°S (*lower line, light shading, right axis*) for the different perturbation scenarios of an early Holocene climate without a baseline flow. The freshwater pulse is introduced at $t = 100$. The *grey lines* represent the five ensemble members of the experiments and the *black line* is the ensemble mean. **a** One-year pulse of 1.63×10^{14} m^3 freshwater. **b** Two-year pulse of 1.63×10^{14} m^3 freshwater. **c** Two-year pulse with 3.26×10^{14} m^3 freshwater. **d** Five-year pulse of 1.63×10^{14} m^3. **e** Five-year pulse of 3.26×10^{14} m^3. **f** Five-year pulse of 4.89×10^{14} m^3

4.4 Comparison between MOC response to freshwater perturbations in EHequi and EHBLF

If we compare the results for the response of the strength of the MOC, the most important difference is the prolonged weakening for the experiments with a baseline flow, while the difference in the minimum value of the maximum North Atlantic overturning is small. The similarity of these minima is related to the Labrador Sea and Irminger Sea being the main areas of deep-water formation that are affected during the first period after the perturbation. The decrease in meridional heat transport at 30°S is similar for the EHequi and EHBLF scenarios, although EHBLF starts from a lower initial value. In both experiments (EHequi and EHBLF) the volume of the freshwater pulse is much more important for the response of the MOC strength than is the duration in which the freshwater is released, at least for the relatively short release durations (i.e. 1, 2 and 5 years) that are tested here.

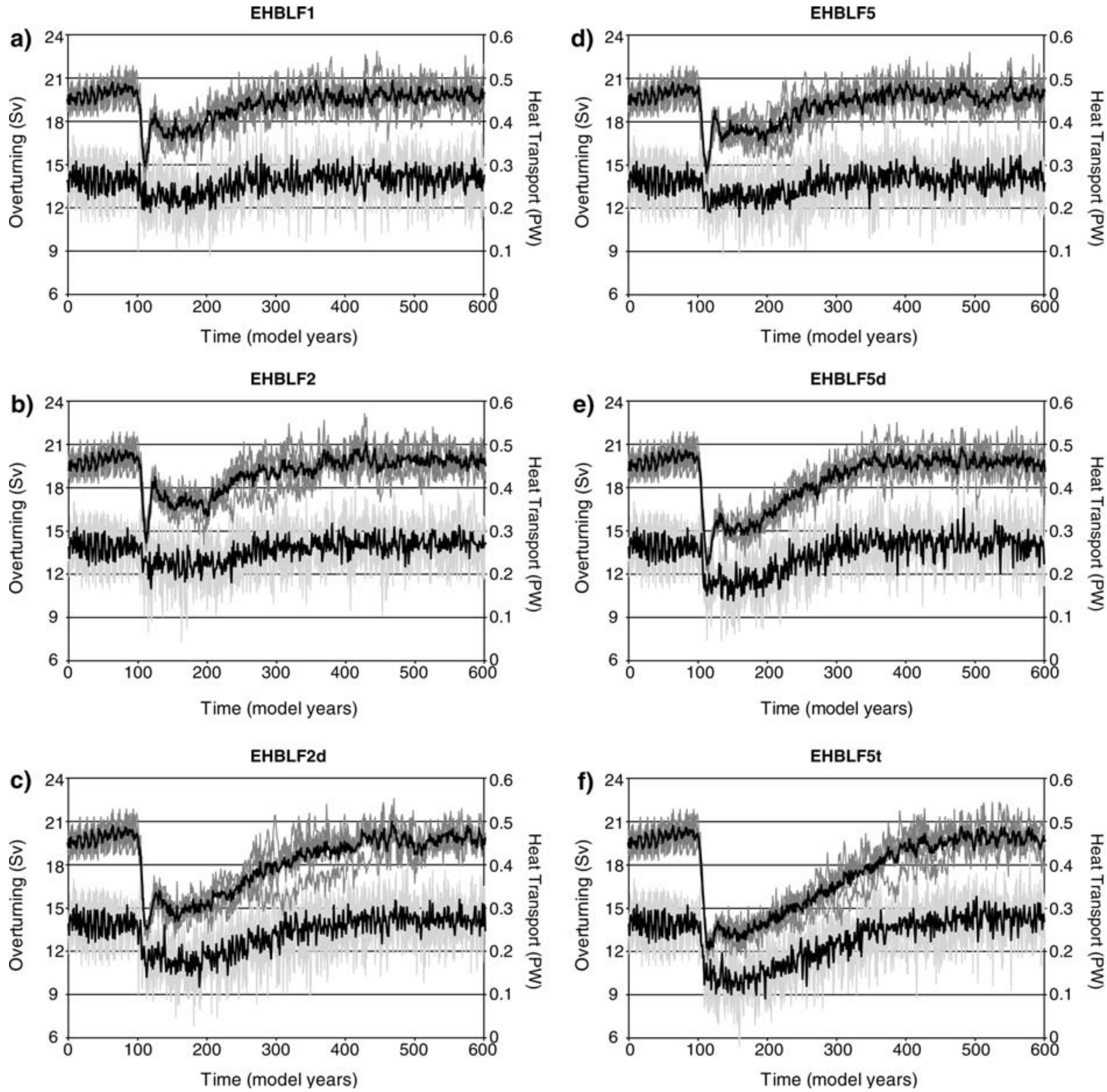

Fig. 4 Maximum North Atlantic overturning (Sv) (*upper line, dark shading, left axis*) and meridional heat transport (PW) in the oceans at 30°S (*lower line, light shading, right axis*) for the different perturbation scenarios of an early Holocene climate with a baseline flow. The freshwater pulse is introduced at $t = 100$. The *grey lines* represent the five ensemble members of the experiments and the *black line* is the ensemble mean. **a** One-year pulse of 1.63×10^{14} m^3 freshwater. **b** Two-year pulse of 1.63×10^{14} m^3 freshwater. **c** Two-year pulse with 3.26×10^{14} m^3 freshwater. **d** Five-year pulse of 1.63×10^{14} m^3. **e** Five-year pulse of 3.26×10^{14} m^3. **f** Five-year pulse of 4.89×10^{14} m^3

The different ensemble members show a slightly higher variability of the response of the MOC strength in the EHBLF experiments, sometimes resulting in a prolonged weakening of more than 100 years (EHBLF2d). However, there is no indication for an intermediate stable state of the MOC as Bauer et al. (2004) and Renssen at al. (2001, 2002) found in their experiments (for differences, see Sect. 6).

5 Discussion: comparison between perturbed EHequi and EHBLF

In this section we explore the response of the climate system to the perturbations in the different experiments in detail by comparing the results of the first ensemble members of EHequi and EHBLF, both perturbed with a 5-year freshwater pulse of double volume. We will refer to these particular experiments as EHequi5d-a and EHBLF5d-a, respectively. Reason for choosing ensemble members from these particular 5-year pulse scenarios is that for both the MOC strength response is clear and century scale, enabling us to analyse the processes involved with the MOC strength weakening. However, since the response of the different ensemble members to the freshwater pulse is very comparable, the succession of events in these particular experiments is also representative for the other ensemble members.

5.1 Response of the ocean

Within two decades after the introduction of the freshwater pulse, overturning in the GIN seas decreases sharply to a value of about two thirds of its pre-perturbed value (Fig. 5a, b). In the EHequi5d-a scenario, a gradual recovery starts immediately 20 years after the perturbation (Fig. 5a), while in the EHBLF5d-a scenario the decreased overturning oscillates around low values for ~30 years before recovering gradually (Fig. 5b). The average value for the overturning in the GIN seas in the control climate is very similar for the two scenarios. As already described in the former section, the overturning in the North Atlantic immediately decreases sharply after the introduction of the freshwater pulse in EHequi5d-a and EHBLF5d-a (Fig. 5c, d). The average value for the maximum North Atlantic overturning in the control climate is ~7 Sv lower in EHBLF5d-a, but the lowest overturning value after the perturbation is only ~2 Sv less than in EHBLF5d-a. After the abrupt weakening, in both experiments the MOC strength intensifies rapidly to values of ~4 Sv lower than the control value, followed by a small weakening again before recovering gradually.

From two time slices, indicated by the dark and light grey shading in Fig. 5, we analysed the temperature anomaly as deviating from the respective control climates (Fig. 6). Please bear in mind that the control climate is different for the two experiments (Fig. 2). For the first 20 years after the introduction of the

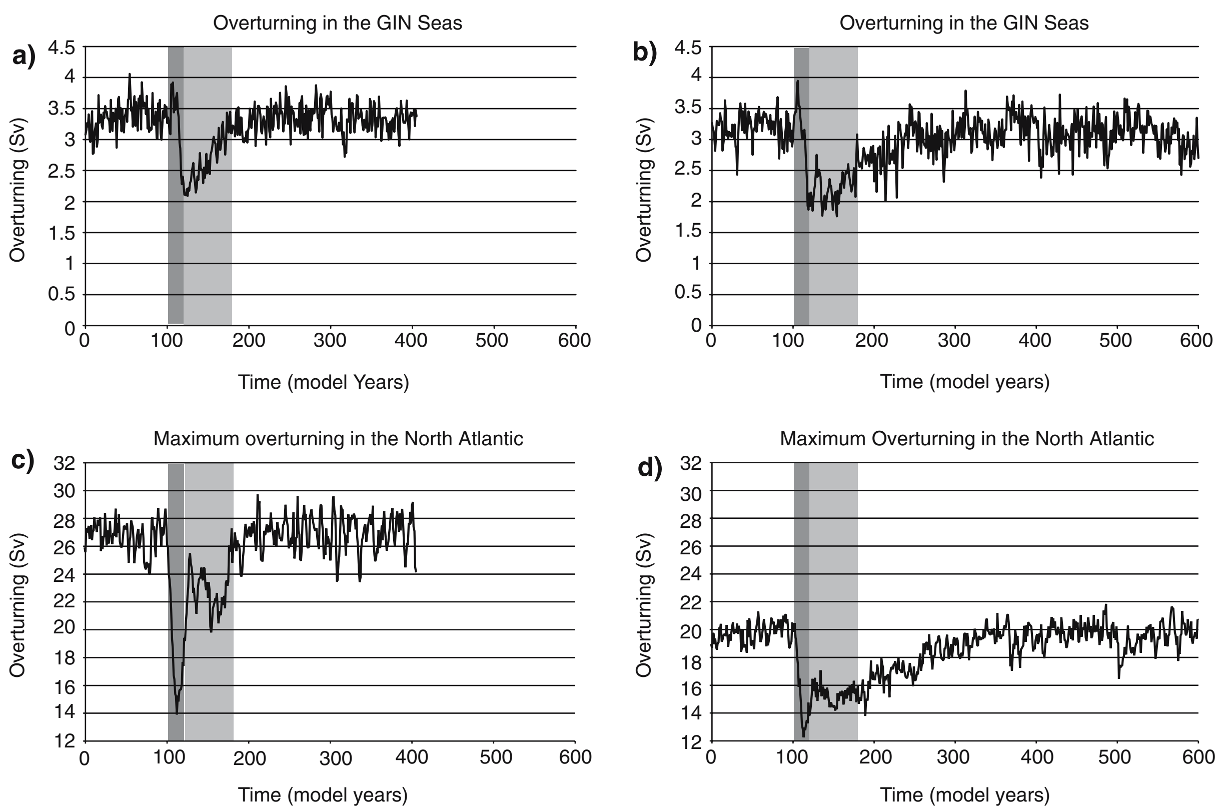

Fig. 5 **a** Overturning in the GIN seas (Sv) for EHequi5d-a. **b** Overturning in the GIN Seas (Sv) for EHBLF5d-a. **c** Maximum North Atlantic Overturning (Sv) for EHequi5d-a. **d** Maximum North Atlantic Overturning (Sv) for EHBLF5d-a. The *shading* indicates the periods for which we plotted mean annual sea surface temperature in Fig. 6. The overturning in the GIN Seas is defined as the maximum of the meridional overturning streamfunction in the GIN Seas after averaging over 1 month (which explains the difference from the values of GIN Sea overturning in the annual mean maximum overturning streamfunction plots in Fig. 1)

freshwater pulse (dark shading in Fig. 5), clear differences exist between the two experiments. Both experiments show a cooling belt from the north of Scandinavia to Iceland that can be explained as a result from reduced convection following the surface freshening (see Sect. 5.2). Surprisingly, in both scenarios, a transient warm anomaly of more than 2°C is present north of Iceland, coinciding with a northward retreat of the ice cover there. This coincides with a shift in convection in the GIN seas in the second decade after the introduction of the freshwater towards a more south-westerly position (not shown), and the subsequent supply of heat to this site, through advection and from the deep-sea to the surface. However, this shift almost does not influence the overall GIN Sea overturning strength (Fig. 5). Differences between the experiments are a warm area south of Greenland in the EHBLF5d-a experiment where in the EHequi5d-a experiment a distinguished cooling is simulated. Again, an increase in convection strength and associated ocean-to-atmosphere heat flux is responsible for this warm anomaly, which is so pronounced since convection was almost absent in the control climate (Fig. 1c). Similarly, the Labrador Sea shows a higher negative temperature anomaly in the EHequi5d-a experiment. These differences show close agreement to the temperature anomalies as observed between the EHequi and EHBLF control climates (Fig. 2), and therefore can be explained by the diminished deep-water formation in the Labrador Sea and the Irminger Sea following the freshwater pulse, which was already greatly diminished in the EHBLF5d-a experiment as a response to the constant adding of freshwater. Finally, a warming is present off the east coast of America, which can be explained by an intensification of the North Atlantic subtropical gyre due to stronger winds during the increasing of the meridional temperature gradient occurring in the first 10 years after introduction of the fresh water pulse. This may also explain the cooler SSTs off Africa.

The SST anomaly for the two experiments during years 20–80 after the introduction of the freshwater pulse (light shading in Fig. 5) is similar, both in magnitude and in spatial distribution (Fig. 6c, d). An exception is the stronger cold anomaly at the southern tip of Greenland in the EHequi5d-a experiment. In both experiments, the main temperature decrease is between Iceland and Greenland with a cooling up to 4°C, while the GIN Sea, Labrador Sea and the Atlantic Ocean south of Greenland cool by around 1°C. The extreme cooling in the Denmark Strait can be attributed to increased sea-ice cover here (not shown). The other cooling sites appear to be less influenced by increased sea-ice cover, and the cooling is caused by reduced convection following the lowering of salinity and subsequent decreased ocean-to-atmosphere heat-flux at these sites.

These results support the idea that the introduction of the baseline flow in the control climate mostly influences the duration of the climate anomaly, and not the magnitude. The difference in control climate, and therefore the shutdown of LSW formation in the EHequi5d-a experiment relative to a control run with LSW formation as opposed to the experiments without baseline flow however, can explain most of the differences between the two experiments.

The 60-year mean SST anomalies of EHequi5d-a and EHBLF5d-a in Fig. 6c, d shows a cooling around the North Atlantic, which is consistent with the spreading of proxy-evidence for the event (Alley et al. 2005; Rohling and Pälike 2005; Wiersma and Renssen 2006). The magnitude of the cooling is smaller than previously modelled (Renssen et al. 2001, 2002; Bauer et al. 2004) and reaches less far south in Western Europe and North America where, averaged over this time period, the cooling does not exceed –0.5°C. Therefore, in the present study, the mean annual temperature averaged over a 60-year period (i.e. between 20 and 80 years after the freshwater pulse) in the EHequi5d-a and EHBLF5d-a scenarios underestimates the cooling as reconstructed from proxy-evidence in Western Europe (Wiersma and Renssen 2006). The simulated cooling of ~1°C in northern Scandinavia is smaller than simulated by Renssen et al. (2001, 2002) and is more consistent with reconstructed Northern Scandinavia summer temperatures that show a decrease by up to 1°C (Korhola et al. 2000, 2002; Seppä and Birks 2001). Therefore, the present model appears to perform better for this crucial region in ocean circulation. Simulated temperatures in this region are mainly controlled by oceanic heat flux to the convection site near Spitzbergen. In model Version 2, the Nordic Seas had a much stronger overturning than in Version 3, imposing a stronger positive feedback and therefore a too strong cooling (Renssen et al. 2001, 2002) when overturning is strongly reduced because of the freshwater perturbation (more details about this point are provided in Sect. 6). In terms of cooling in central Greenland, most experiments show a shorter cooling than the duration of the weakening of the MOC, with a larger variability between the different ensemble members. The scenarios without a baseline flow that are perturbed by a freshwater pulse of, respectively, 1.63×10^{14}, 3.26×10^{14} and 4.89×10^{14} m^3, have an average duration of the cooling in Greenland of respectively 50, 70 and 110 years with corresponding

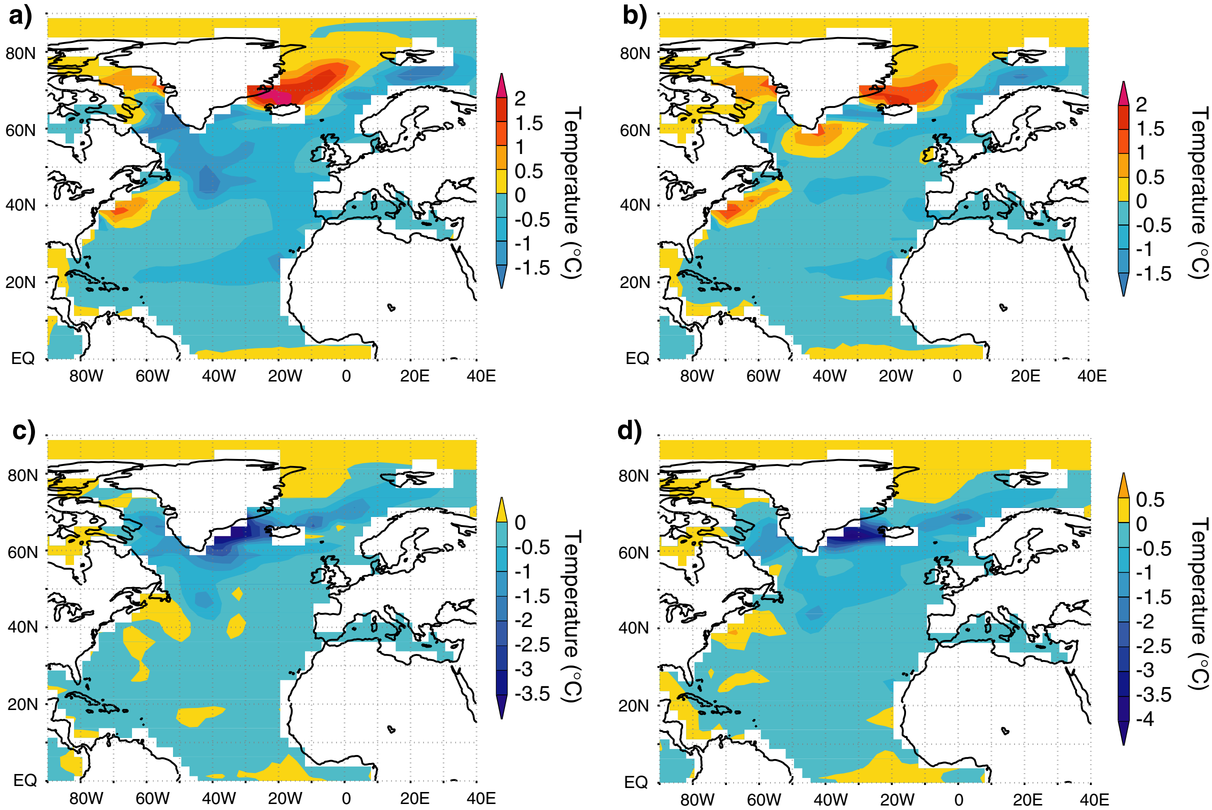

Fig. 6 Maps showing mean annual SST anomalies (°C) as deviating from the control climate for **a** EHequi5d-a and **b** EHBLF5d-a for the first 20 years after the introduction of the freshwater pulse, and **c** EHequi5d-a and **d** EHBLF5d-a for the years 20–80 after the introduction of the freshwater pulse. The periods used are indicated in Fig. 5 as *dark shading* for the first 20 years, and *light shading* for the years 20–80

maximum cooling of 4, 5 and 5°C. Similarly, the scenarios with a baseline flow show an average duration of the cooling of 120, 190 and 260 years for these respective scenarios with corresponding maximum cooling of 4, 5 and 6°C. A recent study estimates the duration of the cooling at ~160 years (Rasmussen et al. 2006), with a magnitude of between 5.4 and 11.7°C (with best estimate of 7.4°C) (Leuenberger et al. 1999) or 6 ± 2°C (Alley et al. 1997). Reasoning backward, to simulate an event of ~160 years with a magnitude that falls within these constraints, in our model a freshwater pulse of between 1.63×10^{14} and 3.26×10^{14} m^3 would have to be applied in the EHBLF scenario.

5.2 Labrador Sea versus GIN Seas

A comparison of time-series of convection depth in the Labrador Sea (Fig. 7, top figures) shows, as expected, that convection depth for the control climate in EHequi5d-a is deeper than in the EHBLF5d-a scenario. With the introduction of the freshwater pulse (at $t = 100$), convection depth decreases dramatically following the decrease in sea surface salinity (Fig. 7a, c), and recovers rapidly as the freshwater pulse stops. Interestingly, after the freshwater pulse, convection depth in the Labrador Sea in EHequi5d-a increases markedly to values more than 200 m deeper than before the perturbation. The timing of the increase in convection depth in the Labrador Sea coincides with the fast removal of the salinity anomaly in the Labrador Sea (Fig. 7a, b) and the fast acceleration of MOC in EHequi5d-a and, although smaller in magnitude, EHBLF5d-a (Fig. 5c, d).

The increase in convection depth is probably caused by the interaction between temperature and salinity in the density of the surface waters of the Labrador Sea. With the introduction of the freshwater pulse, sea surface density rapidly decreases in both scenarios (Fig. 8a, b), until the decrease slows down for around a decade as the scenarios come close to minimum values of ~1,026.4 kg/m^3 in EHequi5d-a and ~1,025.8 kg/m^3 in EHBLF5d-a. From this point on, the two scenarios show a different path. In EHequi5d-a the density rapidly increases as salinity increases, but the temperatures are lower than in the decreasing density trajectory. At $t = 120$ the increase in density slows down and SST becomes colder until $t = 130$. This period with colder SSTs corresponds to the period with deeper convection in Fig. 7a. From this point on, temperatures

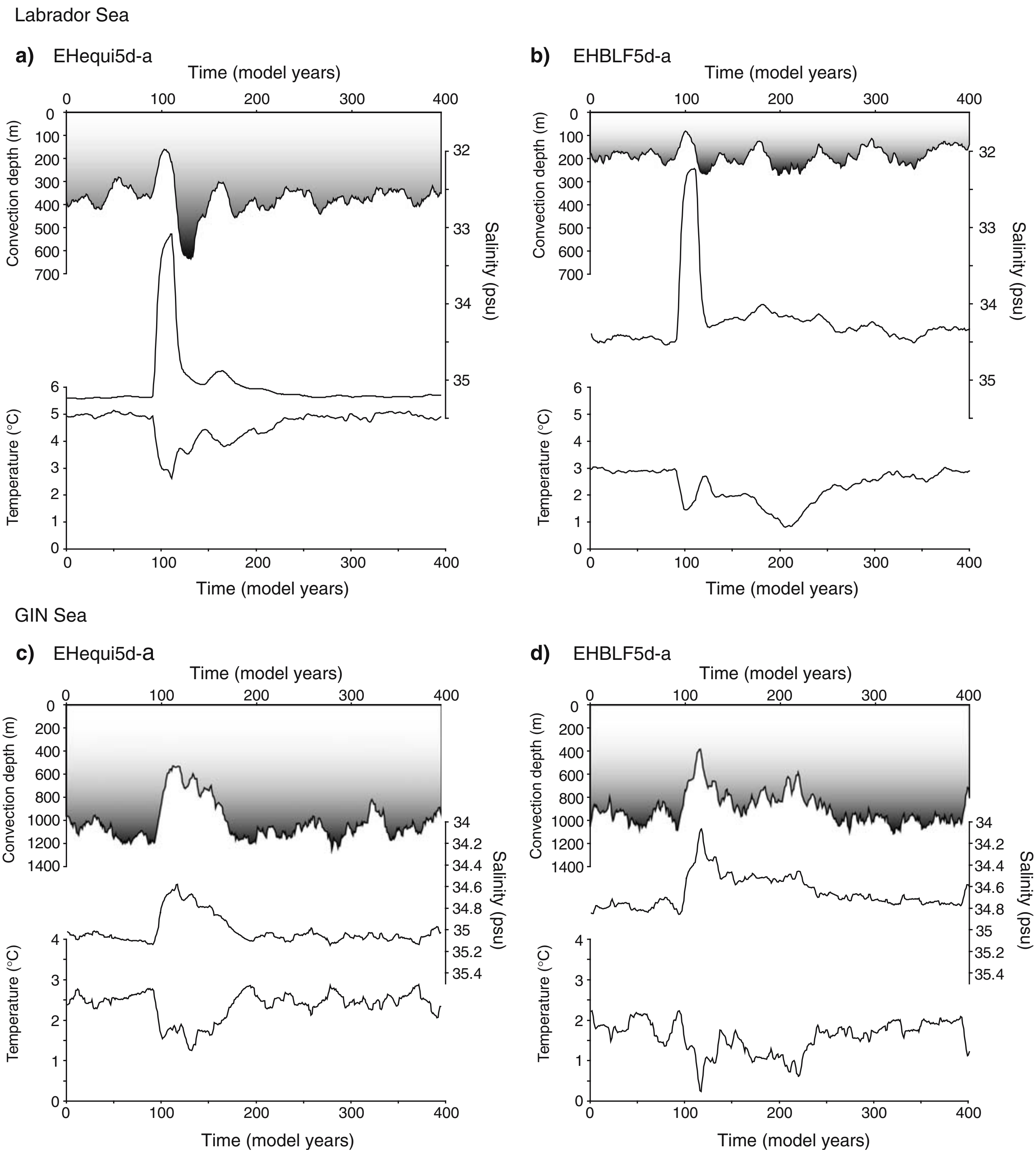

Fig. 7 Twenty-one-year running mean time series of February convection depth (m) (*grey shading*), February sea surface salinity (psu) and February sea surface temperature (°C) in the predominant convection area in the Labrador Sea (between 60 and 50°W and 57 and 63°N, *upper figures*) and the GIN Sea (between 5 and 15°E and 73 and 77°N, *lower figures*) for EHequi5d-a (**a**, **c**) and EHBLF5d-a (**b**, **d**)

and salinities slowly recover to the pre-perturbed values while going through one small additional loop. In EHBLF5d-a, density rapidly increases after the minimum density value is crossed, but with temperatures that are higher than in the decreasing density trajectory. After 20 years, the values are close to pre-perturbed values. From here on, a slow, drifting decrease in temperature occurs for almost 90 years. From $t = 210$, temperatures increase again, drifting slowly towards pre-perturbed state values. In the EHBLF5d-a scenario, the low surface density in the Labrador Sea caused by the baseline flow prevents deep convection to occur. In contrast, in EHequi5d-a a fast increase in density by higher SSS accompanied by a relatively small lowering of SST can cause a decadal scale increase in convection of more than 200 m.

Convection depth in the GIN Sea near Spitzbergen shows a different response to the freshwater pulse (Fig. 7, lower figures). The fresh salinity anomaly is strongly reduced as it arrives at the convection site. Still convection depth rapidly decreases in both experiments, following the SSS changes. The time evolution in the GIN-Sea appears more irregular as a result of a high-frequency variability caused by strong interactions between sea-ice and convection: episodes of increased sea-ice influx freshen the surface waters by melting and reducing local evaporation, thereby reducing surface density that overwhelms the opposite effect of the cooling, and thus produces a reduction in deep convection, as also simulated by Renssen et al. (2005a). In the EHBLF5d-a experiment, this high-frequency variability is larger (causing the more irregular curve) as a result of the lower initial surface temperatures facilitating sea-ice growth and therefore resulting in more frequent sea-ice influx and melting. This is also shown by Fig. 9 showing increased sea-ice transport between Spitzbergen and Norway into the direction of the convection site, especially during the perturbed period in EHBLF5d-a. These more frequently occurring episodes of sea-ice influx prevent fast recovery of the salinity anomaly as they frustrate convection, and therefore stretch the cold period.

The trend of gradual recovery of the density can be attributed to the gradual increase of SSS in the North Atlantic by changes in the surface freshwater balance and transportation and diffusion of the relatively fresh surface water away from this area, and the replacement by advected higher salinity waters from lower latitudes. Several factors may play a role in the slower recovery of the MOC of the EHBLF experiments. In particular, the removal of the surface low salinity waters from the North Atlantic by convection and replacement by advected high-salinity waters (the standard advective salt feedback). As the overturning is already slower, more time is required to recover from the weakened state because it cannot remove freshwater by convection as fast as in the EHequi scenario, and transport more saline water to these convection sites. The deeper

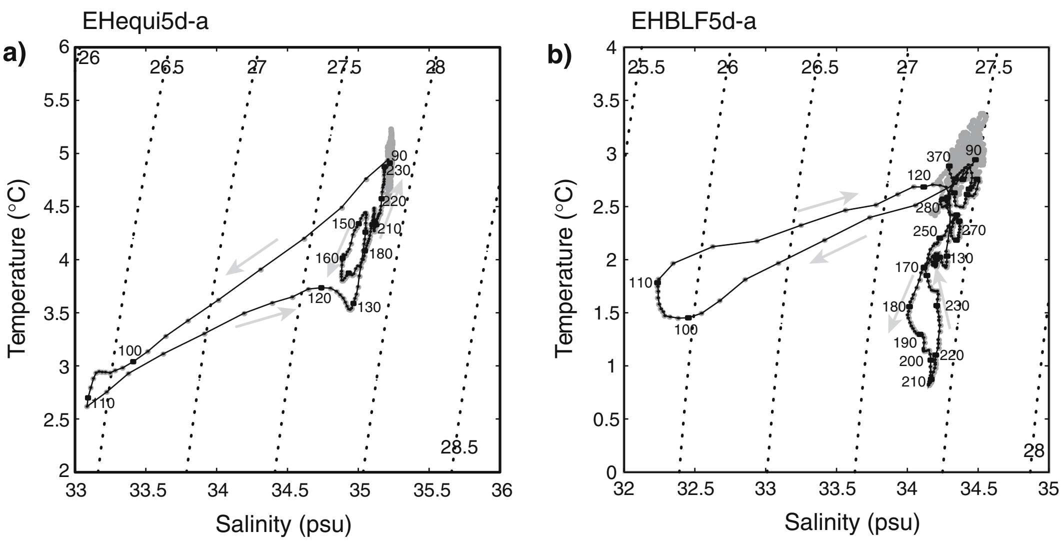

Fig. 8 February SST—SSS plots of the 21-year running mean for the Labrador Sea with corresponding dashed density contours (+1000 kg/m^3) for **a** EHequi5d-a and **b** EHBLF5d-a. The *black dots* connected by the *black line* represent the changes in SST and SSS during the perturbed state of the MOC, with every 10 years a *black square*, if possible labeled with the corresponding year. The *grey dots* represent the SST and SSS changes before and after the perturbed state, showing the models range of natural variability of SST and SSS in the Labrador Sea

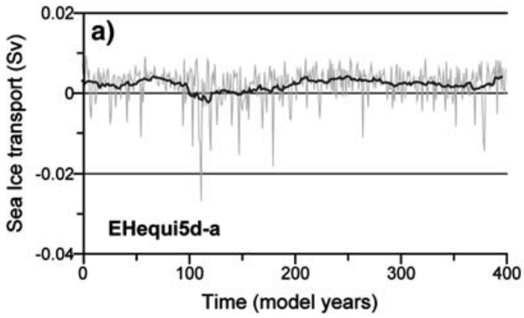

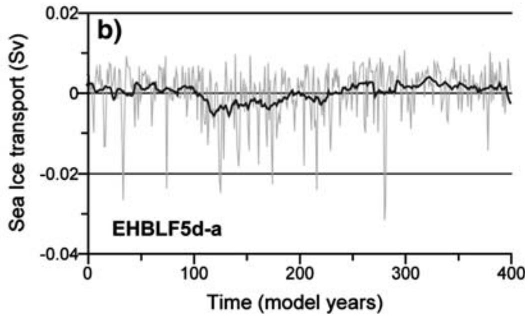

Fig. 9 Twenty-one-year running mean (*black line*) and annual mean (*grey line*) of the sea-ice transport (Sv) between Spitzbergen and Norway, **a** for EHequi5d-a and **b** for EHBLF5d-a. *Negative values* indicate a predominant transport in westward direction (i.e. towards GIN seas convection site)

convection in the Labrador Sea in response to the freshwater pulse in the EHequi scenario may be especially efficient in recovering salinity in the North Atlantic, as relatively fresh water is removed with increased LSW production, and more saline surface waters are advected to the north. Since this convection in the Labrador Sea is suppressed by the constant baseline flow, MOC recovery takes longer in the EHBLF scenario. This hypothesis is consistent with the coincidence in EHequi5d-a of the increase in convection depth in the Labrador Sea, the fast removal of the salinity anomaly there and the fast acceleration of the MOC strength.

The lower temperatures in the control climate of EHBLF and during the MOC slowdown in the GIN Sea may also play a role. The lower temperatures facilitate sea-ice growth and therefore cause an increased chance of sea ice influx at these sites, which prevents convection to occur by the freshening of surface waters and therefore slows down the removal of the salinity anomaly.

In summary, Labrador Sea convection and GIN Sea convection show a different response to the freshwater pulse: both show a decrease in convection depth, but in the Labrador Sea this general decrease is interrupted by a decadal scale increase in EHequi5d-a. In the EHBLF5d-a experiment, the lower surface water density in the Labrador Sea caused by the baseline flow dampens this convection depth increase and in the GIN Seas the slowdown is prolonged due to lower temperatures and more sea-ice interactions. In the Labrador Sea, such a delicate balance between SSS and SST in controlling deep convection has already been observed on longer time scales in proxy-data (Solignac et al. 2004) and in a transient Holocene climate simulation under greenhouse gas and astronomical forcing (Renssen et al. 2005a).

6 Comparison with other model studies

Our study is comparable to previous modelling studies on the 8.2 ka BP event by Renssen et al. (2001, 2002) and Bauer et al. (2004). Renssen et al. (2001, 2002) experimented with a constant volume of 4.67×10^{14} m^3 freshwater that was released with differing durations (10, 20, 50 and 500 years) into the Labrador Sea. These experiments were performed with the previous version of the ECBilt-CLIO climate model that had no representation of LSW formation and a less realistic GIN Seas overturning value. Furthermore the released volume of 4.67×10^{14} m^3 exceeds the highest estimate found in the literature (Törnqvist et al. 2004). In these experiments, the model's MOC shifted to a new unstable state, making the recovery unpredictable as it was governed by high-frequency variability involving the atmosphere. Still, the climate response to the freshwater pulse of one of the 20 years pulse duration experiments did show a good agreement with proxy-evidence (Wiersma and Renssen 2006). In the experiments performed in this study with the ECBilt-CLIO-VECODE Version 3, we found no indication for such an unstable state with the freshwater pulses that were applied. Therefore, in the current experiments high-frequency variability is of minor influence on the duration of the event. In the Renssen et al. (2002) paper, the existence of the unstable state is prolonged by a strong positive feedback by enhanced sea-ice export from the Barents Sea, representing a considerable increase in freshwater transport to the site of convection. In our model we do see enhanced export from the Barents Sea to the site of convection, as described in Sect. 5.2, but to a much lesser extent. This weaker positive feedback in combination with a smaller share of the GIN Sea overturning (17 Sv vs.

3 Sv) in the total North Atlantic overturning may be the reason that such an unstable state is not present in the current experiments, which makes the MOC recovery more predictable.

Bauer et al. (2004) released a volume of 1.6×10^{14} m^3 freshwater into the North Atlantic Ocean between 50 and 70°N in an early Holocene climate. In their experiments with the CLIMBER-2 model, a freshwater baseline flow caused an increased chance of a longer collapse of the MOC to freshwater perturbations. Also in these experiments, the MOC shifted into an unstable climate state, which made the duration of the perturbed state unpredictable. Unfortunately, the CLIMBER-2 model has a coarse spatial resolution, and the ocean basin variables are computed as zonal means for the oceans, making a study on the respective roles of convection in the Labrador Sea and GIN Seas impossible.

The current study suggests that the magnitude and duration of the weakening in overturning circulation is mainly a function of the volume of freshwater released, at least for the scenarios tested here. A similar gradual recovery after a freshwater perturbation was found by Manabe and Stouffer (1995) in an attempt to simulate the Younger Dryas cooling. If these findings are realistic, it means that from knowing the exact volume of freshwater that was released during the lake outburst, new information on the sensitivity to perturbations of the early Holocene climate state can be derived. This would also provide a strong constraint on models and on their representation of the response of the MOC to freshwater release. Unfortunately, the uncertainty on this volume is presently still large, implying that it is possible to find a realistic scenario that reproduces the observed event reasonably well for different model sensitivities.

In our simulations, the presence of a baseline flow from the melting LIS is of great influence on the response of the MOC. This implies that the use of the 8.2 ka BP event in the Paleoclimate-hosing Model Intercomparison Project (PhMIP, Schlessinger 2005) to assess the performance of models is more complex than introducing a short freshwater pulse, and the influence of a baseline flow from the melting LIS should be tested in the models. Furthermore our results show that the Labrador Sea is an important and sensitive player in the global ocean circulation. Other investigators have already suggested that the current freshening in combination with greenhouse warming may well promote the collapse of the LSW formation (Wood et al. 1999; Weaver and Hillaire-Marcel 2004).

7 Summary and conclusions

In this paper we showed the results of freshwater perturbation experiments focused on the early Holocene (8.5 ka BP) climate. First we experimented with the introduction of a realistic baseline flow from the LIS and compared this with proxy data. In this way we obtained two early Holocene reference climate states. Next, to simulate the 8.2 ka BP event, we perturbed these two early Holocene climate states with freshwater pulses varying in volume and duration into the Labrador Sea based on recent estimates constrained by geological evidence. We investigated the response of the MOC and the response of the ocean. From these experiments, we come to the following conclusions:

(1) The simulated early Holocene climate with a baseline flow from the LIS results in ceased convection in the Labrador Sea, and a cold anomaly of ~2°C around the Labrador Sea gradually decreasing to ~1°C in the Irminger Sea, compared to a simulation without a baseline flow. These results are consistent with proxy-data that record absence of LSW formation in the early Holocene.

(2) In all experiments, the MOC intensity weakens sharply, followed by a gradual recovery to pre-perturbed values.

(3) In our experiments, the volume of the freshwater pulse is the dominant factor in the response of the MOC. Duration and timing of the freshwater pulse have almost no effect on the response of the MOC, at least for the relatively short release durations (i.e. 1, 2 and 5 years) that are tested here. This outcome suggests that future research should focus on better estimates on the volume of freshwater that was released. Sea level reconstructions as performed by Törnqvist et al. (2004) provide these estimates as they include the amount of ice that was released together with the freshwater.

(4) The experiments with a baseline flow into the Labrador Sea show a slower recovery of the MOC strength. Therefore, in an early Holocene climate with a baseline flow, less freshwater is needed to produce an event of similar duration than without a baseline flow. This implies that model intercomparison studies covering the 8.2 ka BP event should consider including a representation of a baseline flow in their early Holocene climate state.

(5) By introducing a volume of 1.63×10^{14} m^3, the estimated volume of the Laurentide lakes (Leverington et al. 2002), the maximum simulated

duration of the weakening of the MOC strength is ~160 years. In the experiments without a baseline flow, this volume produces a weakening of only ~100 years. To produce an event in Greenland with a duration of ~160 years and a magnitude, i.e. within the constraints of proxy evidence, in our model, a freshwater pulse of between 1.63×10^{14} and 3.26×10^{14} m^3 would have to be applied in the EHBLF control climate.

(6) In contrast with other modelling studies, no indication is found for an intermediate stable weakened state of the MOC in our model with the freshwater volumes and release durations used in these experiments.

(7) Convection in the Labrador Sea intensifies periodically during the perturbed state of the MOC. In the experiments with a baseline flow this is dampened by the lower density of the surface water, but still present. Since LSW is relatively fresh, this intensification may play a role in the faster recovery of the MOC in experiments without a baseline flow.

References

Alley RB, Mayewski PA, Sowers T, Stuiver M, Taylor KC, Clark PU (1997) Holocene climatic instability—a prominent, widespread event 8200 yr ago. Geology 25:483–486

Alley RB, Agustsdottir AM (2005) The 8k event: cause and consequences of a major Holocene abrupt climate change. Quaternary Sci Rev 24:1123–1149

Barber DC, Dyke A, Hillaire-Marcel C, Jennings AE, Andrews JT, Kerwin MW, Bilodeau G, McNeely R, Southon J, Morehead MD, Gagnon J-M (1999) Forcing of the cold event of 8,200 years ago by catastrophic drainage of laurentide lakes. Nature 400:344–348

Bauer E, Ganopolski A, Montoya M (2004) Simulation of the cold climate event 8200 years ago by meltwater outburst from Lake Agassiz. Paleoceanography 19:PA3014. DOI 10.1029/2004PA001030

Berger A, Loutre MF (1991) Insolation values for the climate of the last 10 million years. Quaternary Sci Rev 10:297–317

Berger A (1992) Orbital variations and insolation database. IGBP PAGES/World Data Center-A for Paleoclimatology Data Contribution Series # 92-007. NOAA/NGDC Paleoclimatology Program, Boulder, CO, USA

Bond GC, Kromer B, Beer J, Muscheler R, Evans MN, Showers W, Hoffmann S, Lotti-Bond R, Hajdas I, Bonani G (2001) Persistent solar influence on north atlantic climate during the holocene. Science 294:2130–2133

Brovkin V, Bendtsen J, Claussen M, Ganopolski A, Kubatzki C, Petoukhov V, Andreev A (2002) Carbon cycle, vegetation, and climate dynamics in the Holocene: experiments with the CLIMBER-2 model. Global Biogeochem Cycles 16(4):1139. DOI 10.1029/2001GB001662

Campin J-M, Goosse H (1999) Parameterization of density-driven downsloping flow for a coarse-resolution oceaan model in z-coordinate. Tellus 51A:412–430

Clarke GKC, Leverington DW, Teller JT, Dyke AS (2004) Paleohydraulics of the last outburst flood from glacial lake agassiz and the 8200 BP cold event. Quaternary Sci Rev 23:389–407

Clarke GKC, Leverington DW, Teller JT, Dyke AS, Marshall SJ (2005) Fresh arguments against the shaw megaflood hypothesis. A reply to comments by David Sharpe on paleohydraulics of the last outburst flood from glacial lake agassiz and the 8200 BP cold event. Quaternary Sci Rev 24:1533–1541

Cottet-Puinel M, Weaver AJ, Hillaire-Marcel C, de Vernal A, Clark PU, Eby M (2004) Variation of labrador sea deep water formation over the last glacial cycle in a climate model of intermediate complexity. Quaternary Sci Rev 23:449–465

Cubasch U, Meehl GA, Boer GJ, Stouffer RJ, Dix M, Noda A, Senior CA, Raper S, Yap KS (2001) Projections of future climate change. in climate change 2001. In: Houghton JT, Ding Y, Griggs DJ, Noguer M, van der Linden PJ, Dai X, Maskell K, Johnson CA (eds) The scientific basis. contribution of working group I to the third assessment report of the intergovernmental panel on climate change. Cambridge University Press, New York, pp 525–582

Deleersnijder E, Campin J-M (1995) On the computation of the barotropic mode of a free-surface world ocean model. Ann Geophys 13:675–688

Dyke AS, Prest VK (1989) Paléogéographie de l'amérique du nord septentrionale, entre 18 000 and 5000 ans avant le présent. Commission géologique du Canada carte, échelle, 1703A, 1/12500000

Dyke AS (2003) An outline of north american deglaciation with emphasis on central and northern Canada. In: Ehlers J (ed) Extent and chronology of quaternary glaciation. Elsevier, Amsterdam, pp 371–406

Elliot M, Labeyrie L, Duplessy J-C (2002) Changes in North Atlantic deep-water formation associated with the dansgaard-oeschger temperature oscillations (60-10 ka). Quaternary Sci Rev 21:1153–1165

Fichefet T, Morales Maqueda MA (1997) Sensitivity of a global sea ice model to the treatment of ice thermodynamics and dynamics. J Geophys Res 102:609–646

Gent JR, McWilliams JC (1990) Isopycnal mixing in ocean general circulation models. J Phys Oceanogr 20:150–155

Goosse H, Fichefet T (1999) Importance of ice-ocean interactions for the global ocean circulation: a model study. J Geophys Res 104:23337–23355

Goosse H, Deleersnijder E, Fichefet T, England MH (1999) Sensitivity of a global coupled ocean-sea ice model to the parameterization of vertical mixing. J Geophys Res 104(C6):13681–13695

Goosse H, Renssen H (2001) On the delayed response of sea ice in the Southern Ocean to an increase in greenhouse gas concentrations. Geophys Res Lett 28:3469–3473

Goosse H, Selten FM, Haarsma RJ, Opsteegh JD (2001) Decadal variability in high northern latitudes as simulated by an intermediate-complexity climate model. Ann Glaciol 33:525–532

Goosse H, Selten FM, Haarsma RJ, Opsteegh JD (2002) A mechanism of decadal variability of the sea-ice volume in the Northern Hemisphere. Clim Dynam 19:61–83. DOI 10.1007/s00382-00001-00209-00385

Goosse H, Selten FM, Haarsma RJ, Opsteegh JD (2003) Large sea-ice volume anomalies simulated in a coupled climate model. Clim Dynam 20:523–536. DOI 510.1007/s00382-00002-00290-00384

Goosse H, Renssen H, Timmermann A, Bradley RS (2005) Internal and forced climate variability during the last millennium: a model-data comparison using ensemble simulations. Quaternary Sci Rev 24(12–13):1345–1360

von Grafenstein U, Erlenkeuser H, Müller J, Jouzel J, Johnsen S (1998) The cold event 8200 years ago documented in oxygen isotope records of precipitation in Europe and Greenland. Clim Dynam 14:73–81

Hillaire-Marcel C, de Vernal A, Bilodeau G, Weaver AJ (2001) Absence of deep-water formation in the Labrador Sea during the last interglacial period. Nature 410:1073–1077

Josenhans HW, Zevenhuizen J (1990) Dynamics of the laurentide ice sheet in Hudson Bay, Canada. Mar Geol 92:1–26

Keigwin LD, Lehman SJ (1994) Deep circulation change linked to heinrich event 1 and younger dryas in a middepth North Atlantic core. Paleoceanography 9(2):185–194

Klitgaard-Kristensen D, Sejrup HP, Haflidason H, Johnsen S, Spurk M (1998) A regional 8200 cal. yr BP cooling event in northwest Europe, induced by final stages of the laurentide ice-sheet deglaciation? J Quaternary Sci 13:165–169

Knutti R, Flückinger J, Stocker TF, Timmermann A (2004) Strong hemispheric coupling of glacial climate through freshwater discharge and ocean circulation. Nature 430:851–856

Korhola A, Weckström J, Holmström L, Erästö P (2000) A quantitative holocene climatic record from diatoms in northern fennoscandia. Quaternary Res 54:284–294

Korhola A, Vasko K, Toivonen HTT, Olander H (2002) Holocene temperature changes in northern fennoscandia reconstructed from chironomids using Bayesian modelling. Quaternary Sci Rev 21:1841–1860

Leuenberger MC, Lang C, Schwander J (1999) Delta^{15}N measurements as a calibration tool for the paleothermometer and gas-ice age differences: a case study for the 8200 BP event in GRIP ice. J Geophys Res 104(18):22163–22170

Leverington D, Mann JD, Teller JT (2002) Changes in bathymetry and volume of glacial lake agassiz between 9200 and 7700 14C yr BP. Quaternary Res 57:244–252. DOI 210-1006/qres-2001-2311

Licciardi JM, Teller JT, Clark PU (1999) Freshwater routing of the laurentide ice sheet during the last deglaciation. In: Clark PU, Webb RS, Keigwin LD (eds) Mechanisms of Global climate change at millennial time scales. American Geophysical Union, Washington, DC. Geophys Monogr 112:177–201

Manabe S, Stouffer RJ (1995) Simulation of abrupt climate change induced by freshwater input to the North Atlantic Ocean. Nature 378:165–167

Manabe S, Stouffer RJ (1997) Coupled ocean-atmosphere model response to freshwater input: comparison to younger dryas event. Paleoceanography 12:321–336

Mellor GL, Yamada T (1982) Development of a turbulence closure model for geophysical fluid problems. Rev Geophys Space Phys 20:851–875

Moros M, Emeis K, Risebrobakken B, Snowball I, Kuijpers A, McManus J, Jansen E (2004) Sea surface temperatures and ice rafting in the Holocene North Atlantic: climate influences on northern Europe and Greenland. Quaternary Sci Rev 23:2113–2126

Opsteegh JD, Haarsma RJ, Selten FM, Kattenberg A (1998) ECBILT: a dynamic alternative to mixed boundary conditions in ocean models. Tellus 50A:348–367

Peltier WR (1994) Ice age paleotopography. Science 265:195–201

Rasmussen SO, Andersen KK, Svensson AM, Steffensen JP, Vinther BM, Clausen HB, Siggaard-Andersen M-L, Johnsen SJ, Larsen LB, Dahl-Jensen D, Bigler M, Röthlisberger R, Fischer H, Goto-Azuma K, Hansson ME, Ruth U (2006) A new Greenland ice core chronology for the last glacial termination. J Geophys Res 111:D06102. DOI 10.1029/2005JD006079

Raynaud D, Barnola J-M, Chappellaz J, Blunier T, Indermühle A, Stauffer B (2000) The ice record of Greenhouse gases: a view in the context of future changes. Quaternary Sci Rev 19:9–17

Renssen H, Goosse H, Fichefet T, Campin J-M (2001) The 8.2 kyr BP event simulated by a global atmosphere–sea-ice–ocean model. Geophys Res Lett 28:1567–1570

Renssen H, Goosse H, Fichefet T (2002) Modeling the effect of freshwater pulses on the early Holocene climate: the influence of high frequency climate variability. Paleoceanography 17:1020. DOI 1010.1029/2001PA000649

Renssen H, Goosse H, Fichefet T (2005a) Contrasting trends in North Atlantic deep-water formation in the labrador sea and nordic seas during the holocene. Geophys Res Lett 32:L08711. DOI 08710.01029/02005GL022462

Renssen H, Goosse H, Fichefet T, Brovkin V, Driesschaert E, Wolk F (2005b) Simulating the holocene climate evolution at northern high latitudes using a coupled atmosphere-sea ice-ocean-vegetation model. Clim Dynam 24(1):23–43

Rohling EJ, Pälike H (2005) Centennial-scale climate cooling with a sudden cold event around 8,200 years ago. Nature 434:975–979

Rossow WB, Walker AW, Beuschel DE, Roiter MD (1996) International satellite cloud climatology project (ISCCP) documentation of new cloud datasets. World Meteorological Organisation, Geneva, WMO/TD-No 737

Schaeffer M, Selten FM, Opsteegh JD, Goosse H (2002) Intrinsic limits to predictability of abrupt regional climate change in IPCC SRES scenarios. Geophys Res Lett 29(16):1767. DOI 10.1029/2002GL015254

Schlessinger M (2005) Proposal for PMIP2/1ACE Paleo-hosing Model Intercomparison Project (PhMIP). WUN-ACE Kick-Off Meeting 15th–18th May 2005 (Abstracts)

Seppä H, Birks HJB (2001) July mean temperature and annual precipitation trends during the holocene in the fennoscandian tree-line area: pollen-based climate reconstructions. Holocene 11:527–539

Sharpe D (2005) Comments on: paleohydraulics of the last outburst flood from glacial lake agassiz and the 8200 BP cold event by Clarke et al [Quaternary Sci Rev 23(2004):389–407]. Quaternary Sci Rev 24:1529–1532

Solignac S, de Vernal A, Hillaire-Marcel C (2004) Holocene sea-surface conditions in the North Atlantic—contrasted trends and regimes in the western and eastern sectors (Labrador Sea vs. Iceland Basin). Quaternary Sci Rev 23:319–334

Stocker TF, Wright DG (1991) Rapid transitions of the ocean's deep circulation induced by changes in surface water fluxes. Nature 351:729–732

Teller JT, Leverington DW, Mann JD (2002) Freshwater outbursts to the oceans from glacial Lake Agassiz and their role in climate change during the last deglaciation. Quaternary Sci Rev 21:879–887

Törnqvist TE, Bick SJ, González JL, van der Borg K, de Jong AFM (2004) Tracking the sea-level signature of the 8.2 ka cooling event: new constraints from the mississippi delta. Geophys Res Lett 31:L23309. DOI 23310.21029/22004GL021429

Upham W (1896) The glacial lake agassiz. Monographs of the United States geological survey, vol. 25. Washington Government Printing Office, Washington

Veillette JJ (1994) Evolution and paleohydrology of glacial lakes Barlow and Ojibway. Quaternary Sci Rev 13:945–971

Vellinga M, Wood RA (2002) Global climatic impacts of a collapse of the Atlantic thermohaline circulation. Clim Change 54:251–267

de Vernal (1997) Researchers look for links among paleoclimate events. Eos 78:247–249

Weaver AJ, Hillaire-Marcel C (2004) Global warming and the next ice age. Science 304:400–402

Wiersma AP, Renssen H (2006) Model-data comparison for the 8.2 ka BP event: confirmation of a forcing mechanism by catastrophic drainage of laurentide lakes. Quaternary Sci Rev 25:63–88

Wood RA, Keen AB, Mitchell JFB, Gregory JM (1999) Changing spatial structure of the thermohaline circulation in response to atmospheric CO2 forcing in a climate model. Nature 399:572–575